PERGAMON

Chemical Engineering Science 56 (2001) 6249–6258

Chemical Engineering Science

www.elsevier.com/locate/ces

Eulerian simulations of bubble columns operating at elevated pressures in the churn turbulent flow regime

R. Krishna *, J. M. van Baten

Department of Chemical Engineering, University of Amsterdam, Nieuwe Achtergracht 166, 1018 WV Amsterdam, The Netherlands

Abstract

This paper develops a CFD model for bubble column reactors operating at elevated pressures in the churn-turbulent flow regime. The bubble column is considered to be made up of three phases: (1) liquid, (2) "small" bubbles and (3) "large" bubbles and the Eulerian description is used for each of these phases. Interactions between both bubble populations and the liquid are taken into account in terms of momentum exchange, or drag, coefficients, which differ for the "small" and "large" bubbles. The drag coefficient for the "small" bubbles is determined from the Mendelson correlation (A.I.Ch.E.J., 13 (1967) 250). For determining the drag coefficient of the "large" bubbles, the model of Krishna et al. (Chem. Eng. Sci., 54 (1999a) 171) was used, after correcting for the influence of elevated pressure on the large bubble rise velocity. The interactions between the large and small bubble phases are ignored. The turbulence in the liquid phase is described using the $k-\varepsilon$ model. The three-phase description of bubble columns was implemented within the Eulerian framework of a commercial code CFX 4.2 of AEA Technology, Harwell, UK. Simulations using the cylindrical coordinate system (assuming axi-symmetry) showed good agreement with experimental data on gas holdup obtained in a 0.15 m diameter column by Letzel et al. (Chem. Eng. Sci., 52 (1997) 3733). The Eulerian simulations predict that the liquid circulation velocities increase with increased system pressures; this result is in consonance with the liquid phase mixing experiments of Wilkinson et al. (Chem. Eng. Sci., 49 (1993) 5735).

Keywords: Bubble columns; Large bubbles; Small bubbles; Churn-turbulent flow regime; Bubble rise velocity; Backmixing; Pressure influence; Computational fluid dynamics

1. Introduction

Bubble column reactors used in industry are often operated at elevated pressures and high superficial gas velocities at which the churn-turbulent flow regime prevails. Such reactors can have diameters as large as 6–10 m (Sie & Krishna, 1999). Experimental laboratory studies on bubble columns are often restricted to columns smaller than about 0.3 m in diameter (Deckwer, 1992). Furthermore, there is only a limited number of experimental studies on bubble columns operated at elevated pressures (Fan, Yang, Lee, Tsuchiya, & Luo, 1999; Letzel, Schouten, van den Bleek, & Krishna, 1997, 1998, 1999; Reilly, Scott, De Bruijn, & MacIntyre, 1994; Wilkinson, Spek, & van Dierendonck, 1992).

The influence of elevated pressure on bubble column hydrodynamics is very significant, as is evidenced by the published experimental results of Letzel et al. (1997, 1998, 1999) for gas hold-up measured in a bubble column of 0.15 m diameter with the system nitrogen–water; see Fig. 1. For example, their experimental data show that for operation at a superficial gas velocity $U=0.2$ m/s, the gas hold-up ε increases from a value of 0.29 at $p=0.1$ MPa to a value which is about twice as large for operation at $p=1$ MPa; see Fig. 1(b).

The observed increase in the gas hold-up with increasing pressures is due to two reasons. Firstly, increased pressure delays the onset of churn-turbulent flow, i.e. the superficial gas velocity at which regime transition occurs, U_{trans}, increases with increasing p; see Fig. 1(c). The physical explanation for the delay in the regime transition with increased system pressure, which is equivalent with increasing gas density ρ_G, is to be found in the reduced probability of propagation of instabilities leading to delayed flow regime transition (Krishna, De Swart, Hennephof, Ellenberger, & Hoefsloot, 1994). As shown in Fig. 1(c), the correlation of Reilly et al. (1994) adequately describes the increase of U_{trans} with gas

* Corresponding author. Tel.: +31-20-525-7007; fax: +31-20-525-5604.

E-mail address: krishna@its.chem.uva.nl (R. Krishna).

0009-2509/01/$ - see front matter
PII: S0009-2509(01)00274-3

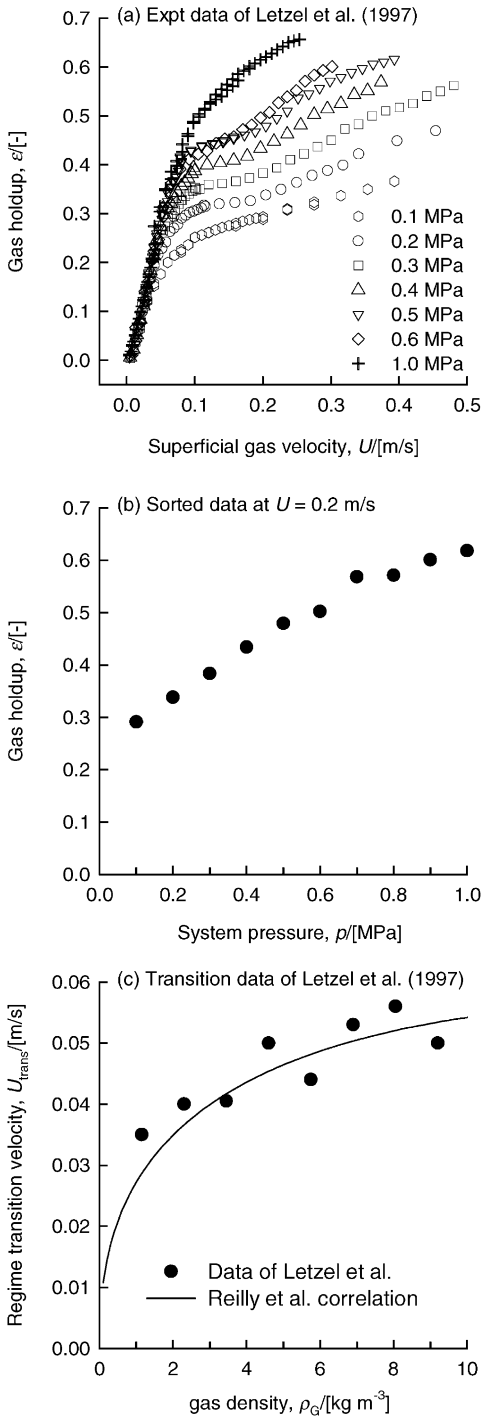

Fig. 1. Experimental data of Letzel et al. (1997) for gas holdup and regime transition velocity.

density ρ_G. Using Kelvin–Helmoltz stability analysis, Letzel et al. (1998) showed that there is a second influence of increased system pressures, that of decrease in the stability of large bubbles. The break-up of large bubbles, with increasing pressures, leads to a significant decrease in the rise velocity of the large bubble population.

Though correlations have been published for estimating the gas hold-up, mixing and mass transfer in bubble columns operating at elevated pressures (Reilly et al., 1994; Wilkinson et al., 1992), such correlations have never been tested for columns larger than 0.15 m in diameter. It is now well established that bubble column hydrodynamics is a strong function of the column diameter (Krishna & Ellenberger, 1996; Krishna, Urseanu, van Baten, & Ellenberger, 1999b). The rules for scaling up of high-pressure bubble column reactors to commercial scale are largely unknown.

Experimentation on a large scale at elevated pressures is prohibitively expensive and is only carried out by large corporations (Sie & Krishna, 1999).

Several recent publications have established the potential of computational fluid dynamics (CFD) for describing the hydrodynamics of bubble columns (Grevskott et al., 1996; Jakobsen, Sannæs, Grevskott, & Svendsen, 1997; Krishna et al., 1999b; Lapin & Lübbert, 1994; Pan, Dudukovic, & Chang, 2000; Sanyal, Vasquez, Roy, & Dudukovic, 1999; Sokolichin & Eigenberger, 1994, 1999). Eulerian simulations have been used with some degree of success for describing the scale influence of bubble columns (Krishna, van Baten, & Urseanu, 2000). All published CFD models have been tested and validated only for operations at atmospheric pressure. The major objective of the present work is to develop an Eulerian simulation model for bubble columns operating at elevated pressures. We focus on the churn-turbulent regime of operation. The developed model is validated with the published experimental data in a 0.15 m diameter column (Wilkinson et al., 1992).

2. Development of CFD model

For the homogeneous regime of operation of bubble columns a more or less uniform bubble size is obtained. In the churn-turbulent regime of operation the bubble sizes vary over a wide range between 1 and 50 mm depending on the operating conditions and phase properties. The rise characteristics of the bubbles depend on its size and liquid phase properties. Our approach for modelling purposes is to assume that in the churn-turbulent flow regime we have two distinct bubble classes: "small" and "large"; see Fig. 2. The small bubbles are in the size range of 1–6 mm and are either spherical or ellipsoidal in shape depending the physical properties of the liquid (Clift, Grace, & Weber, 1978; Fan & Tsuchiya, 1990). The large bubbles are typically in the range of 20–80 mm range (De Swart, van Vliet, & Krishna, 1996) and fall into the spherical cap regime. These bubbles undergo frequent coalescence and break-up. The rise velocities of the large bubbles can approach 2 m/s and has been found to be significantly scale dependent (Krishna & Ellenberger, 1996) and because of the severe bypassing effect, these bubbles largely

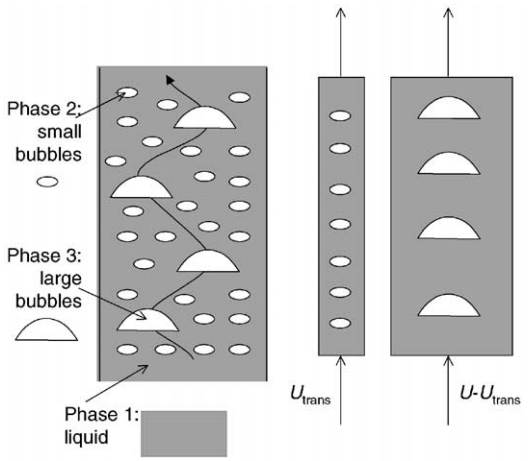

Fig. 2. Three-phase model for bubble columns operating in the churn-turbulent regime; adapted from Krishna and Ellenberger (1996).

determine the gas phase conversion. In conformity with the Krishna–Ellenberger model, we assume that the superficial gas velocity through the small bubble phase corresponds to that at the regime transition point, U_{trans}. The transition velocity can be estimated using the Reilly et al. (1994) correlation or provided as model input. As shown in Fig. 1(c), the Reilly et al. (1994) correlation adequately describes the variation of U_{trans} with increasing ρ_G.

For each of the three phases shown in Fig. 2 the volume-averaged mass and momentum conservation equations in the Eulerian framework are given by

$$\frac{\partial(\varepsilon_k\rho_k)}{\partial t} + \nabla\cdot(\rho_k\varepsilon_k\mathbf{u}_k) = 0, \tag{1}$$

$$\frac{\partial(\rho_k\varepsilon_k\mathbf{u}_k)}{\partial t} + \nabla\cdot(\rho_k\varepsilon_k\mathbf{u}_k\mathbf{u}_k - \mu_k\varepsilon_k(\nabla\mathbf{u}_k + (\nabla\mathbf{u}_k)^{\mathrm{T}})) = -\varepsilon_k\nabla p + \mathbf{M}_{kl} + \rho_k\mathbf{g}, \tag{2}$$

where ρ_k, $\mathbf{u}_k$, ε_k and μ_k represent, respectively, the macroscopic density, velocity, volume fraction and viscosity of the kth phase, p is the pressure, $\mathbf{M}_{kl}$, the interphase momentum exchange between phase k and phase l and $\mathbf{g}$ is the gravitational force.

The momentum exchange between either bubble phase (subscript b) and liquid phase (subscript L) phases is given by

$$\mathbf{M}_{L,b} = \frac{3}{4}\rho_L\frac{\varepsilon_b}{d_b}C_D(\mathbf{u}_b - \mathbf{u}_L)|\mathbf{u}_b - \mathbf{u}_L|. \tag{3}$$

The liquid phase exchanges momentum with both the "small" and "large" bubble phases. No interchange between the "small" and "large" bubble phases have been included in the present model and each of the dispersed bubble phases exchanges momentum only with the liquid phase. The neglect of the interactions between the small and large bubble populations has been verified by Vermeer and Krishna (1981). The interphase drag coefficient is calculated from equation:

$$C_D = \frac{4}{3}\frac{\rho_L - \rho_G}{\rho_L}gd_b\frac{1}{V_b^2}, \tag{4}$$

where V_b is the rise velocity of the appropriate bubble population. We have only included the drag force contribution to $\mathbf{M}_{L,b}$, in keeping with the works of Sanyal et al. (1999) and Sokolichin and Eigenberger (1999). The added mass force has been ignored in the present analysis. The reason for this neglect is because the focus of the simulations and experiments in this work is on the churn-turbulent flow regime. The distinguishing feature of this regime is the existence of large fast-rising bubbles. These large bubbles do not have a closed wake and the concept of added mass is not applicable. The small bubbles on the other hand do have a closed wake. However, in the churn-turbulent flow regime these bubbles suffer strong recirculations, moving downwards near the wall region. Inclusion of the added mass contributions to the small bubbles led to severe convergence difficulties. The added mass contributions were therefore omitted. Lift forces are also ignored in the present analysis because of the uncertainty in assigning values of the lift coefficients to the small and large bubbles. For the large bubbles, for which Eö > 40 holds, literature data suggest the use of a negative lift coefficient, whereas for small bubbles for which typically Eö $= 2$, the lift coefficient is positive (Jakobsen et al., 1997).

For the continuous, liquid, phase, the turbulent contribution to the stress tensor is evaluated by means of $k-\varepsilon$ model, using standard single phase parameters $C_\mu = 0.09$, $C_{1\varepsilon} = 1.44$, $C_{2\varepsilon} = 1.92$, $\sigma_k = 1$ and $\sigma_\varepsilon = 1.3$. Our implementation of the $k-\varepsilon$ model does not include any further modifications for say buoyancy effects. The applicability of the $k-\varepsilon$ model implementation has been verified by the recent work of Sokolichin and Eigenberger (1999). No turbulence model is used for calculating the velocity fields inside the dispersed "small" and "large" bubble phases.

From visual observations of bubble column operations with the air–water system, the small bubbles were observed to be in the 3–6 mm size range. The rise velocity of air bubbles is practically independent of bubble diameter in this size range and the Mendelson (1967) equation for the rise velocity:

$$V_{b,\text{small}} = \sqrt{2\sigma/\rho_L d_b + gd_b/2} \tag{5}$$

is used in the simulation model developed here. Fig. 3 compares experimental data of Krishna, Urseanu, van Baten, and Ellenberger (1999c) on the rise velocity of single gas bubbles in the 2–10 mm range with the Mendelson (1967) and Harmathy (1960) correlations. It is seen

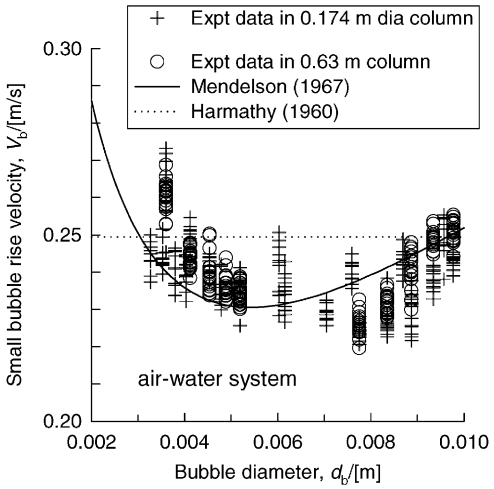

Fig. 3. Small bubble rise velocity in air–water system. Experimental data of Krishna et al. (1999c) compared with the Mendelson (1967) and Harmathy (1960) correlations.

that Eq. (5) provides a good representation of the experimental data.

In order to determine the large bubble rise velocity, we use the model developed earlier by Krishna, Urseanu, van Baten and Ellenberger (1999a), which introduces an acceleration factor AF into the Collins (1967) relation for the rise of a single spherical cap bubble:

$$V_{b,\mathrm{large}} = 0.71\sqrt{g d_{b,\mathrm{large}}}(\mathrm{SF})(\mathrm{AF}). \tag{6}$$

The expressions developed by Krishna et al. (1999a) for the large bubble size and acceleration factor for air–water systems have been obtained from experimental data obtained at atmospheric pressure conditions. Recent work of Letzel et al. (1998) has shown that the large bubble rise velocity decreases with increasing gas density. We therefore modify the model of Krishna et al. (1999a) for the large bubble rise velocity by introducing a correction factor to account for the influence of elevated pressures:

$$V_{b,\mathrm{large}} = 0.71\sqrt{g d_{b,\mathrm{large}}}(\mathrm{SF})(\mathrm{AF})(\mathrm{DF}), \tag{7}$$

where DF is the density correction factor. For air at atmospheric conditions used in the experiments, $\rho_G = 1.29\ \mathrm{kg/m^3}$ and the density correction factor is unity, i.e. $\mathrm{DF} = 1$. For any gas at any system pressure, having a gas density ρ_G, the density correction factor can be calculated from

$$\mathrm{DF} = \sqrt{1.29/\rho_G}. \tag{8}$$

The model developed above has been verified by comparison with experimental data by Krishna, Urseanu, and Dreher (2000).

A commercial CFD package CFX 4.2 of AEA Technology, Harwell, UK, was used to solve the equations of continuity and momentum. This package is a finite volume solver, using body-fitted grids. The grids are non-staggered and all variables are evaluated at the cell centres. An improved version of the Rhie and Chow (1983) algorithm is used to calculate the velocity at the cell faces. The pressure-velocity coupling is obtained using the SIMPLEC algorithm (van Doormal & Raithby, 1984). For the convective terms in Eqs. (1) and (2) hybrid differencing was used. A fully implicit backward differencing scheme was used for the time integration.

3. Simulation results and comparison with experimental data

Simulations were carried out for a column of 0.15 m diameter with the nitrogen–water system operating at 0.1, 0.2, 0.3, 0.4, 0.5 and 0.6 MPa. The parameters used in the simulations are as specified in Table 1. The superficial gas velocity through the small bubble phase is taken to be U_{trans}. The remainder of the gas ($U - U_{\mathrm{trans}}$) was taken to rise up the column in the form of large bubbles. This implies that at the distributor the "large" bubbles constitute a fraction $(U - U_{\mathrm{trans}})/U$ of the total incoming volumetric flow, whereas the "small" bubble constitute a fraction (U_{trans}/U) of the total incoming flow. All simulations were carried out using cylindrical axi-symmetry with the grid specified in Fig. 4. The total column height was taken to be 6 m. The number of grid cells in the radial and axial directions were 20 and 300, respectively, making a total of 6000 cells. In all the simulations the column was first filled with water to a height of 2.5 m and at time $t = 0$, air was introduced at the specified superfical velocity, U, at the bottom of the column. The time stepping strategy used in the transient simulations for attainment of steady state was typically: 100 steps at 5×10^{-5} s, 100 steps at 1×10^{-4} s, 100 steps at 5×10^{-4} s, 100 steps at 1×10^{-3} s, 200 steps at 3×10^{-3} s, 1400 steps at 5×10^{-3} s, 8000 steps at 1×10^{-2} s. The simulations were carried out on either a Silicon Graphics Power Indigo workstation with the R8000 processor or Silicon Graphics Power Challenge workstation with R10,000 processor. Each simulation was completed in about five days. Typical transient development of the velocities of the liquid, small and large bubbles at a position 2.5 m above the distributor are shown in Fig. 5(a) for $p = 0.2$ MPa, $U = 0.1$ m/s. When steady state is established, the cumulative gas hold-up can be determined along the column height. A typical profile of the cumulative gas hold-up is shown in Fig. 5(b). All the gas hold-up data reported in this paper correspond to the cumulative gas hold-up at a height of 2.5 m above the distributor.

Table 1
Parameter values for Eulerian simulations of bubble column operating at elevated pressures. Column diameter = 0.15 m; Total column height = 6 m; Initial liquid height = 2.5 m; Reported hydrodynamics are at the monitoring height of 2.5 m; Gas density at atmospheric pressure = 1.29 kg/m^3; Liquid phase is water ($\rho_L = 998$ kg/m^3; $\mu_L = 0.001$ Pa s; $\sigma = 0.072$ N/m)

Pressure (MPa)	U (m/s)	U_{trans} (m/s)	$d_{b,\text{small}}$ (m)	$d_{b,\text{large}}$ (m)	$C_{D,\text{small}}$	$C_{D,\text{large}}$
0.2	0.1	0.032	0.004	0.025	0.937	0.632
	0.15	0.032	0.004	0.031	0.937	0.591
	0.2	0.032	0.004	0.035	0.937	0.548
	0.25	0.032	0.004	0.039	0.937	0.508
	0.3	0.032	0.004	0.042	0.937	0.471
	0.35	0.032	0.004	0.045	0.937	0.437
0.3	0.1	0.04	0.004	0.024	0.936	0.954
	0.15	0.04	0.004	0.03	0.936	0.896
	0.2	0.04	0.004	0.035	0.936	0.832
	0.25	0.04	0.004	0.038	0.936	0.77
	0.3	0.04	0.004	0.042	0.936	0.714
	0.35	0.04	0.004	0.44	0.936	0.663
0.4	0.1	0.045	0.004	0.023	0.935	1.277
	0.15	0.045	0.004	0.03	0.935	1.201
	0.2	0.045	0.004	0.034	0.935	1.116
	0.25	0.045	0.004	0.038	0.935	1.034
	0.3	0.045	0.004	0.041	0.935	0.958
	0.35	0.045	0.004	0.044	0.935	0.889
0.5	0.1	0.048	0.004	0.023	0.933	1.598
	0.15	0.048	0.004	0.029	0.933	1.506
	0.2	0.048	0.004	0.034	0.933	1.4
	0.25	0.048	0.004	0.038	0.933	1.296
	0.3	0.048	0.004	0.041	0.933	1.201
	0.35	0.048	0.004	0.044	0.933	1.115
0.6	0.1	0.05	0.004	0.022	0.932	1.918
	0.15	0.05	0.004	0.029	0.932	1.81
	0.2	0.05	0.004	0.034	0.932	1.682
	0.25	0.05	0.004	0.038	0.932	1.558
	0.3	0.05	0.004	0.041	0.932	1.444
	0.35	0.05	0.004	0.044	0.932	1.34

The Eulerian simulations show that the gas hold-up increases with increasing system pressure; see Fig. 6(a). This is in agreement with the experimental data shown in Fig. 1(a). Data sets at each pressure when compared in Figs. 6(b)–(f) show reasonably good agreement between simulations and experiment.

The major advantage of the CFD approach is that besides the total gas holdup, complete information is obtained on the hydrodynamics of bubble columns. Fig. 7(a) shows the radial liquid velocity profiles $V_L(r)$ for $U = 0.2$ m/s and various system pressures. The simulations show an increase in the centre-line velocity $V_L(0)$ with increasing p; see Fig. 7(b). For comparison purposes, the centre-line liquid velocity data of Hills (1974) for an air–water bubble column of 0.14 m diameter at 0.1 MPa is also shown in Fig. 7(b). Firstly, we note that there is reasonably good agreement between the Hills experimental data and the Eulerian simulations for $p = 0.2$ MPa. This gives us some confidence in the simulation results for $V_L(0)$. The increase of $V_L(0)$ with increasing p as observed in the simulations (cf. Fig. 7(b)) is, however, not an expected result but can be rationalised as follows. The drag coefficient of the large bubbles increases with increasing p; see Table 1. This means that the momentum exchange between the large bubbles and the liquid becomes more intense with increasing pressure, resulting in an increase in the liquid circulation velocity. There is no published information on the influence of increased system pressures on the liquid circulation velocities; such information is necessary for direct verification of the simulation trends.

Wilkinson, Haringa, Stokman, and van Dierendonck (1993) have measured the axial dispersion coefficient,

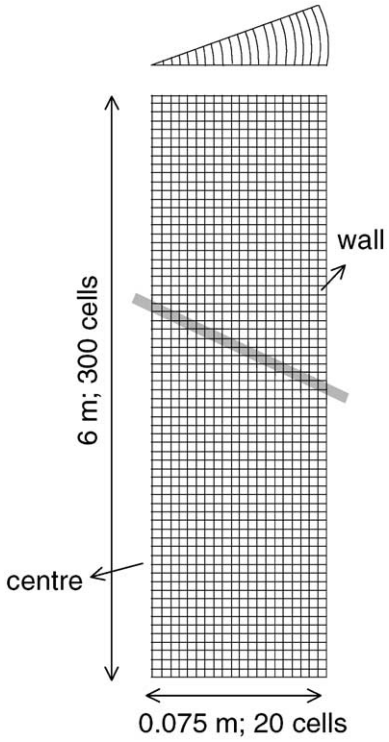

Fig. 4. Grid used in the 2D cylindrical axi-symmetric simulations.

$D_{ax,L}$, of the liquid phase in a nitrogen–water bubble column of 0.15 m diameter at pressures ranging from 0.1 to 1.5 MPa. Their experimental results show that $D_{ax,L}$ increases with increasing system pressures; see Fig. 8(a). These authors have stressed that their experimental results are not predicted by any of the available literature correlations. In our previous study (Krishna et al., 1999b) we had shown that the axial dispersion coefficient $D_{ax,L}$ can be estimated from a knowledge of the centre-line velocity by use of the correlation

$$D_{ax,L} = 0.31\, V_L(0) D_T. \tag{9}$$

The validity of Eq. (9) has also been established by fully three-dimensional Eulerian simulations of bubble columns by van Baten and Krishna (2001). Eq. (9) may also be applied to high pressure bubble columns provided we take proper account of the influence of the system pressure on the centre-line velocity $V_L(0)$. For any given pressure and superficial gas velocity the CFD simulation results for $V_L(0)$ are given in Fig. 7(b). In Fig. 8(b) we have used Eq. (9) to calculate $D_{ax,L}$ for various system pressures using the $V_L(0)$ simulation results from Fig. 7(b). In conformity with the trends observed by Wilkinson et al. (1993) the simulations show an increase in $D_{ax,L}$ with increasing system pressure. The rate of increase, however, decreases with increasing p, again in conformity with the observations of Wilkinson et al. (1993). It is also heartening to note that the values of

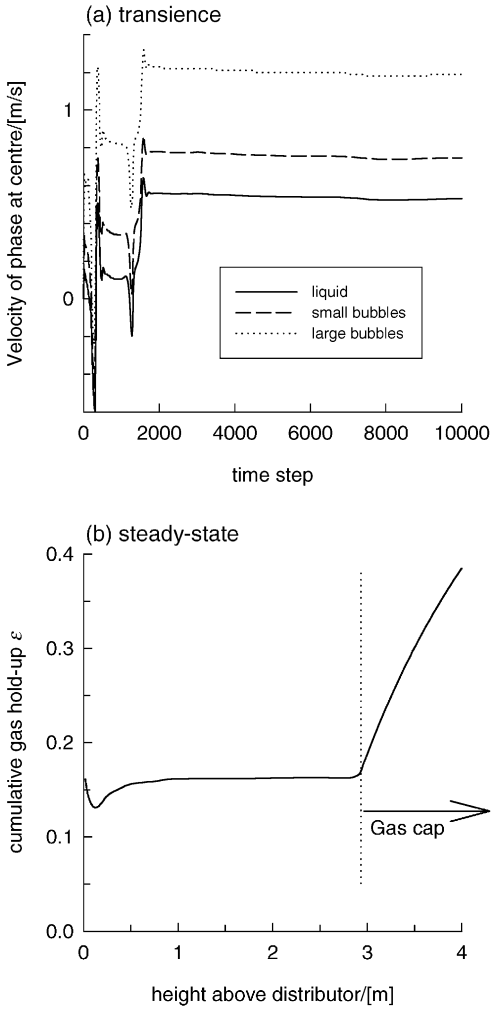

Fig. 5. (a) Transient velocity monitored at height 2.5 m above distributor for $p = 0.2$ MPa, $U = 0.1$ m/s. (b) Cumulative gas hold-up at steady state.

$D_{ax,L}$ estimated from Eulerian simulations at 0.5 MPa agree quite well in with those measured experimentally by Wilkinson et al; see Fig. 8(c).

4. Conclusions

An Eulerian simulation model has been developed for bubble column reactors operated at elevated pressures in the churn-turbulent flow regime. The appropriate drag relation for the "large" bubble population has been derived by introducing a density correction factor into the large bubble rise velocity model of Krishna et al. (1999a). The Eulerian simulations of the gas hold-up are in reasonably good agreement with the experimental data of Letzel et al. (1997) and show significant in ε with increasing p. Our simulations also predict an increase in the liquid circulation velocity, and liquid phase backmixing, with increasing p. The predicted trends are supported

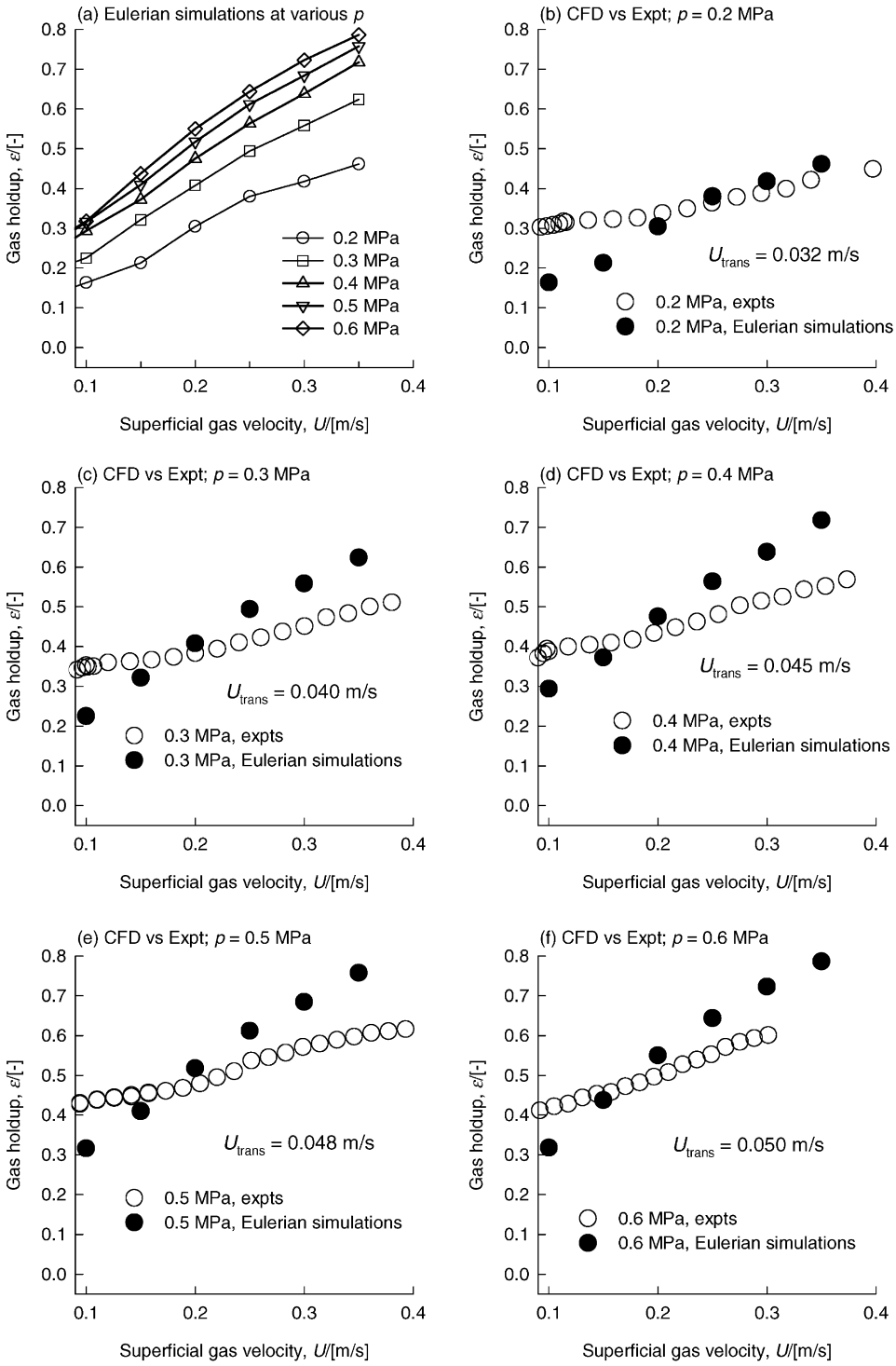

Fig. 6. Comparison of Eulerian simulations for gas hold-up with experimental data of Letzel et al. (1997) for operation of an air–water bubble column at pressures ranging from 0.2 to 0.6 MPa.

by the liquid phase backmixing data of Wilkinson et al. (1993).

Our Eulerian simulation model has only been tested with experimental data on one scale. There is need for further verification of scaling up potential of our model.

Notation

AF	acceleration factor, dimensionless
C_D	drag coefficient, dimensionless
d_b	diameter of either bubble population, m

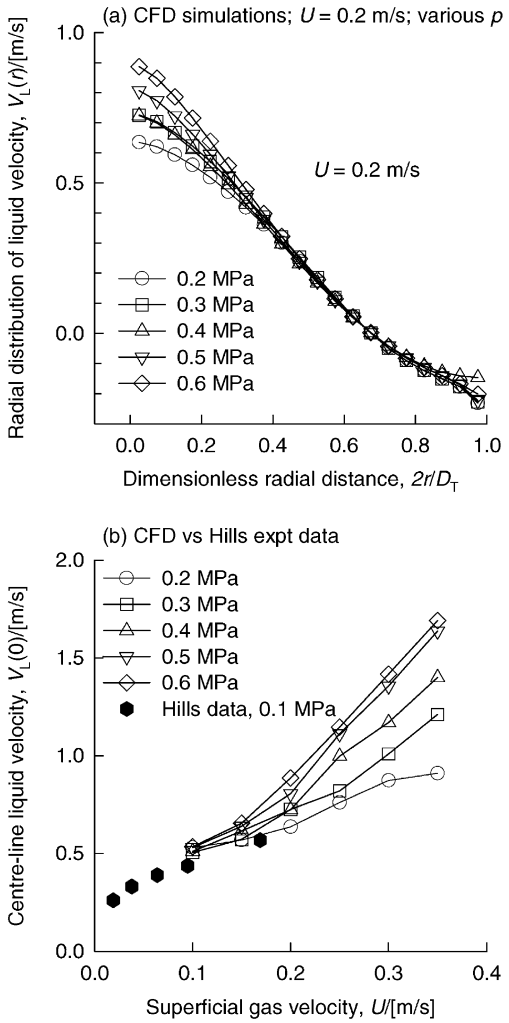

Fig. 7. (a) Radial distribution of liquid velocity $V_L(r)$ for $U = 0.2$ m/s and for various system pressures. (b) Centre-line liquid velocity $V_L(0)$ from Eulerian simulations at various system pressures. Also shown is the experimental data of Hills (1974) at $p = 0.1$ MPa.

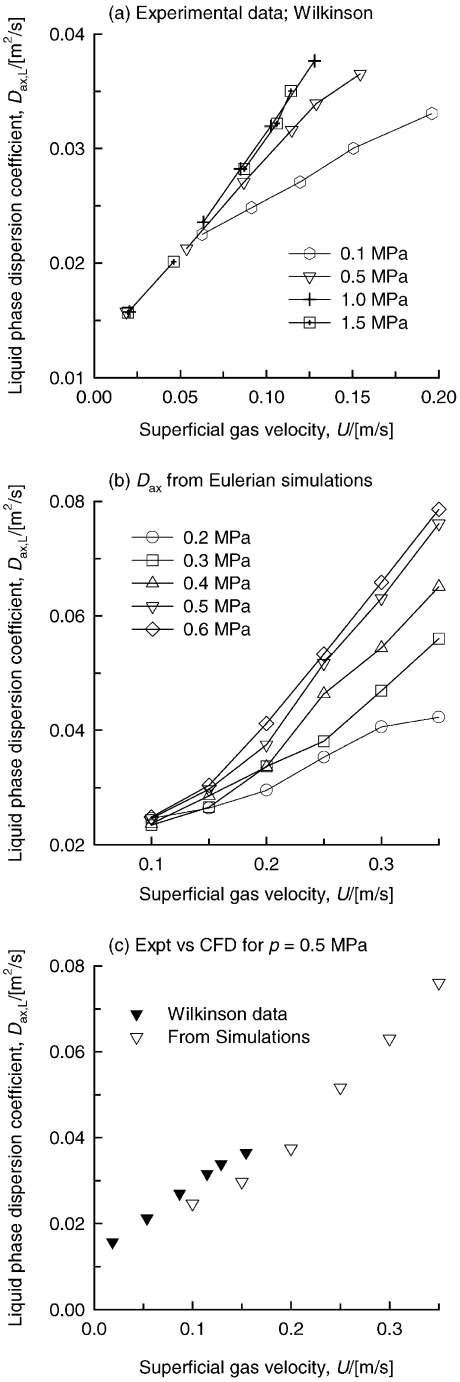

Fig. 8. (a) Experimental data of Wilkinson for axial dispersion coefficient in liquid phase showing influence of pressure on D_{ax}. (b) Axial dispersion coefficient estimated from Eulerian simulations using Eq. (9). (c) Comparison of Wilkinson data with CFD simulation results for D_{ax} at $p = 0.5$ MPa.

$D_{ax,L}$	axial dispersion coefficient of the liquid phase, m^2/s
D_T	column diameter, m
DF	density correction factor, dimensionless
Eö	Eötvös number, $g(\rho_L - \rho_G)d_b^2/\sigma$
g	gravitational acceleration, 9.81 m/s^2
M	interphase momentum exchange term, N/m^3
p	system pressure, Pa
r	radial coordinate, m
SF	scale factor, dimensionless
t	time, s
u	velocity vector, m/s
U	superficial gas velocity, m/s
U_{trans}	superficial gas velocity at regime transition, m/s
$V_L(0)$	centre-line liquid velocity, m/s

Greek letters

ε	total gas hold-up, dimensionless
ε_{trans}	gas hold-up at the regime transition point, dimensionless
μ_L	viscosity of liquid phase, Pa s

ρ density of phase, kg/m^3
σ surface tension of liquid phase, N/m^1

Subscripts

b referring to either bubble population
G referring to gas
L referring to liquid
large referring to the large bubble population
small referring to the small bubble population
trans referring to the transition point
T tower or column

Acknowledgements

The Netherlands Organisation for Scientific Research (NWO) is gratefully acknowledged for providing financial assistance in the form of a "programmasubsidie".

References

van Baten, J. M., & Krishna, R. (2001). Eulerian simulations for determination of the axial dispersion of liquid and gas phases in bubble columns operating in the churn-turbulent regime. *Chemical Engineering Science*, *56*, 503–512.

Clift, R., Grace, J. R., & Weber, M. E. (1978). *Bubbles, drops and particles*. San Diego: Academic Press.

Collins, R. (1967). The effect of a containing cylindrical boundary on the velocity of a large gas bubble in a liquid. *Journal of Fluid Mechanics*, *28*, 97–112.

Deckwer, W. D. (1992). *Bubble column reactors*. New York: Wiley.

De Swart, J. W. A., van Vliet, R. E., & Krishna, R. (1996). Size, structure and dynamics of "large" bubbles in a 2-D slurry bubble column. *Chemical Engineering Science*, *51*, 4619–4629.

Fan, L. S., & Tsuchiya, K. (1990). *Bubble wake dynamics in liquids and liquid–solid suspensions*. Boston: Butterworth-Heinemann.

Fan, L. S., Yang, G. Q., Lee, D. J., Tsuchiya, K., & Luo, X. (1999). Some aspects of high-pressure phenomena of bubbles in liquids and liquid–solid suspensions. *Chemical Engineering Science*, *54*, 4681–4709.

Grevskott, S., Sannæs, B. H., Dudukovic, M. P., Hjarbo, K. W., & Svendsen, H. F. (1996). Liquid circulation, bubble size distributions, and solids movement in two- and three-phase bubble columns. *Chemical Engineering Science*, *51*, 1703–1713.

Harmathy, T. J. (1960). Velocity of large drops and bubbles in media of infinite or restricted extent. *American Institute of Chemical Engineers Journal*, *6*, 281–288.

Hills, J. H. (1974). Radial non-uniformity of velocity and voidage in a bubble column. *Transactions of the Institution of Chemical Engineers*, *52*, 1–9.

Jakobsen, H. A., Sannæs, B. H., Grevskott, S., & Svendsen, H. F. (1997). Modeling of bubble driven vertical flows. *Industrial and Engineering Chemistry Research*, *36*, 4052–4074.

Krishna, R., De Swart, J. W. A., Hennephof, D. E., Ellenberger, J., & Hoefsloot, H. C. J. (1994). Influence of increased gas density on the hydrodynamics of bubble column reactors. *American Institute of Chemical Engineers Journal*, *40*, 112–119.

Krishna, R., & Ellenberger, J. (1996). Gas hold-up in bubble column reactors operating in the churn-turbulent flow regime. *American Institute of Chemical Engineers Journal*, *42*, 2627–2634.

Krishna, R., Urseanu, M. I., van Baten, J. M., & Ellenberger, J. (1999a). Rise velocity of a swarm of large gas bubbles in liquids. *Chemical Engineering Science*, *54*, 171–183.

Krishna, R., Urseanu, M. I., van Baten, J. M., & Ellenberger, J. (1999b). Influence of scale on the hydrodynamics of bubble columns operating in the churn-turbulent regime: Experiments vs. Eulerian simulations. *Chemical Engineering Science*, *54*, 4903–4911.

Krishna, R., Urseanu, M. I., van Baten, J. M., & Ellenberger, J. (1999c). Wall effects on the rise of single gas bubbles in liquids. *International Commnunications in Heat & Mass Transfer*, *26*, 781–790.

Krishna, R., van Baten, J. M., & Urseanu, M. I. (2000). Three-phase Eulerian simulations of bubble column reactors operating in the churn-turbulent flow regime: A scale up strategy. *Chemical Engineering Science*, *55*, 3275–3286.

Krishna, R., Urseanu, M. I., & Dreher, A. (2000). Gas hold-up in bubble columns: Influence of alcohol addition versus operation at elevated pressures. *Chemical Engineering and Processing*, *39*, 371–378.

Lapin, A., & Lübbert, A. (1994). Numerical simulation of the dynamics of two-phase gas–liquid flows in bubble columns. *Chemical Engineering Science*, *49*, 3661–3674.

Letzel, H. M., Schouten, J. C., van den Bleek, C. M., & Krishna, R. (1997). Influence of elevated pressure on the stability of bubbly flows. *Chemical Engineering Science*, *52*, 3733–3739.

Letzel, M. H., Schouten, J. C., van den Bleek, C. M., & Krishna, R. (1998). Influence of gas density on the large-bubble holdup in bubble column reactors. *American Institute of Chemical Engineers Journal*, *44*, 2333–2336.

Letzel, H. M., Schouten, J. C., Krishna, R., & van den Bleek, C. M. (1999). Gas holdup and mass transfer in bubble column reactors operated at elevated pressure. *Chemical Engineering Science*, *54*, 2237–2246.

Mendelson, H. D. (1967). The prediction of bubble terminal velocities from wave theory. *American Institute of Chemical Engineers Journal*, *13*, 250–253.

Pan, Y., Dudukovic, M. P., & Chang, M. (2000). Numerical investigation of gas-driven flow in 2-D bubble columns. *American Institute of Chemical Engineers Journal*, *46*, 434–449.

Reilly, I. G., Scott, D. S., De Bruijn, T. J. W., & MacIntyre, D. (1994). The role of gas phase momentum in determining gas hold-up and hydrodynamic flow regimes in bubble column operations. *Canadian Journal of Chemical Engineering*, *72*, 3–12.

Rhie, C. M., & Chow, W. L. (1983). Numerical study of the turbulent flow past an airfoil with trailing edge separation. *AIAA Journal*, *21*, 1525–1532.

Sanyal, J., Vasquez, S., Roy, S., & Dudukovic, M. P. (1999). Numerical simulation of gas–liquid dynamics in cylindrical bubble column reactors. *Chemical Engineering Science*, *54*, 5071–5083.

Sie, S. T., & Krishna, R. (1999). Fundamentals and selection of advanced Fischer–Tropsch reactors. *Applied Catalysis A*, *186*, 55–70.

Sokolichin, A., & Eigenberger, G. (1994). Gas–liquid flow in bubble columns and loop reactors: Part I. Detailed modelling and numerical simulation. *Chemical Engineering Science*, *49*, 5735–5746.

Sokolichin, A., & Eigenberger, G. (1999). Applicability of the standard—turbulence model to the dynamic simulation of bubble columns: Part I. Detailed numerical simulations. *Chemical Engineering Science*, *54*, 2273–2284.

van Doormal, J., & Raithby, G. D. (1984). Enhancement of the SIMPLE method for predicting incompressible flows. *Numerical Heat Transfer*, *7*, 147–163.

Vermeer, D. J., & Krishna, R. (1981). Hydrodynamics and mass transfer in bubble columns operating in the churn-turbulent

regime. *Industrial and Engineering Chemistry Process Design & Development*, *20*, 475–482.

Wilkinson, P. M., Spek, A. P., & van Dierendonck, L. L. (1992). Design parameters estimation for scale-up of high-pressure bubble columns. *American Institute of Chemical Engineers Journal*, *38*, 544–554.

Wilkinson, P. M., Haringa, H., Stokman, F. P. A., & van Dierendonck, L. L. (1993). Liquid mixing in a bubble column under pressure. *Chemical Engineering Science*, *48*, 1785–1791.